

Supporting Information

Two-dimensional covalent organic framework-based hybrid nanosheet for electrochemical detection of 5-fluorouracil and uracil in biofluids

Jia Liu,^{a,b} Zhiyang Wang,^{a,b,c} Xiaowei Wu, *^{a,b} Shanyue Wei,^{b,d} Yiming Xie,^d Jing Chen ^{a,b} and Can-Zhong Lu *^{a,b,c}

^a CAS Key Laboratory of Design and Assembly of Functional Nanostructures, Fujian Provincial Key Laboratory of Nanomaterials, Fujian Institute of Research on the Structure of Matter, Chinese Academy of Sciences, Fuzhou 350002, China.

^b Xiamen Key Laboratory of Rare Earth Photoelectric Functional Materials, Xiamen Institute of Rare Earth Materials, Haixi Institutes, Chinese Academy of Sciences, Xiamen 361021, China.

^c University of Chinese Academy of Sciences, Beijing 100049, China.

^d Engineering Research Center of Environment-Friendly Function Materials, Ministry of Education, College of Materials Science & Engineering, Huaqiao University, Xiamen 361021, China.

Supporting Figures

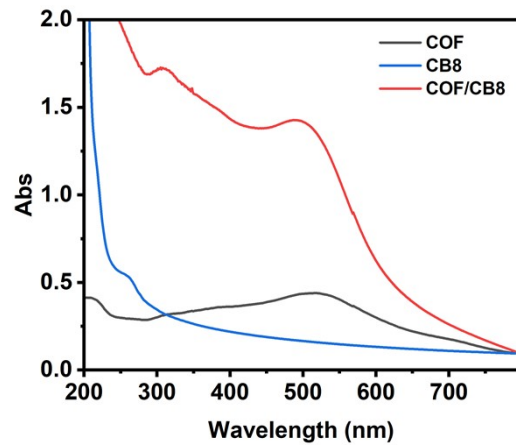


Fig. S1. UV-vis spectra of COF, CB8, and COF/CB8.

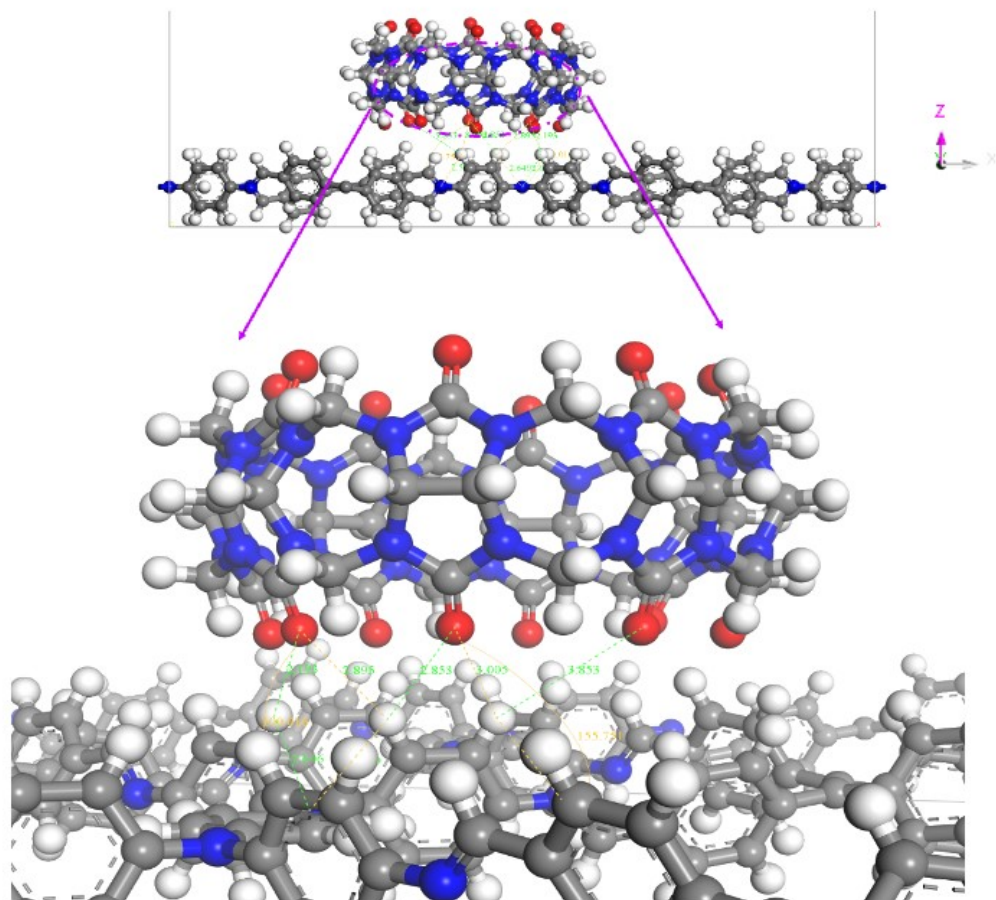


Fig. S2. Potential intermolecular interactions between COF and CB8.

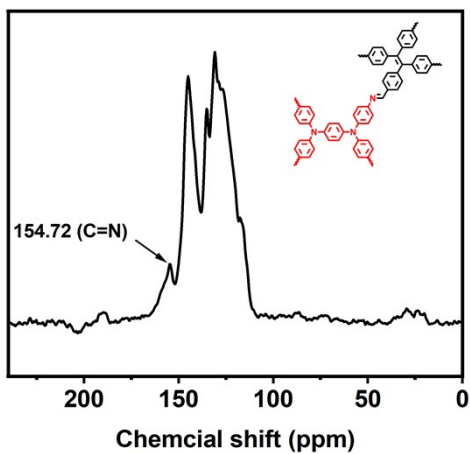


Fig. S3. Solid-state ^{13}C CP-MAS NMR spectrum of COF.

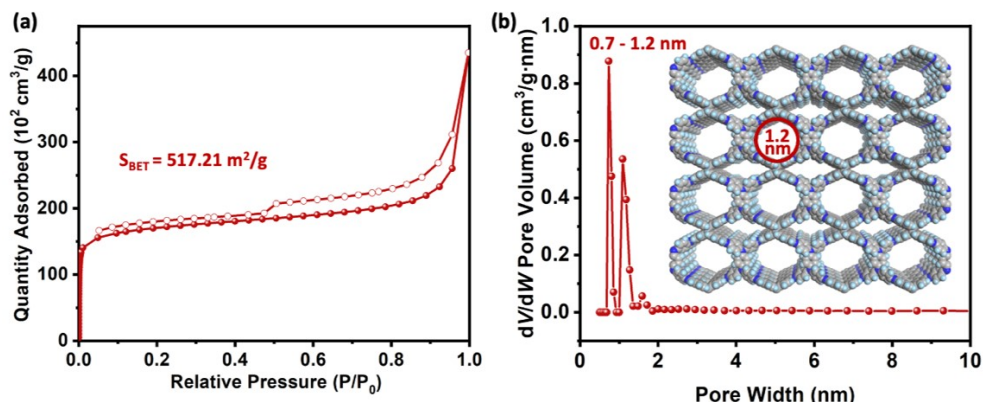


Fig. S4. (a) Nitrogen adsorption-desorption isotherms and (b) pore width distribution of COF.

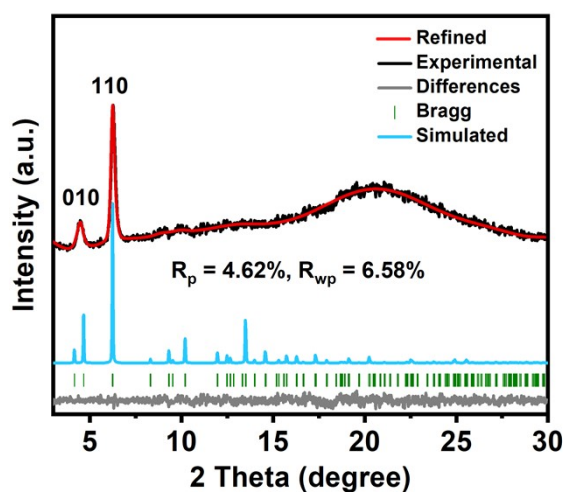


Fig. S5. Experimental and simulated PXRD patterns of COF.

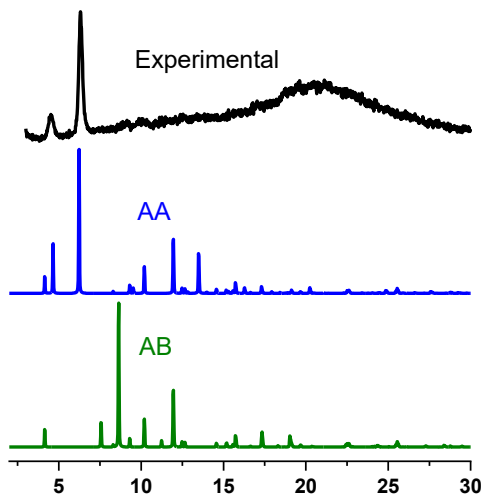


Fig. S6. PXRD patterns of AA and AB stacking of COF.

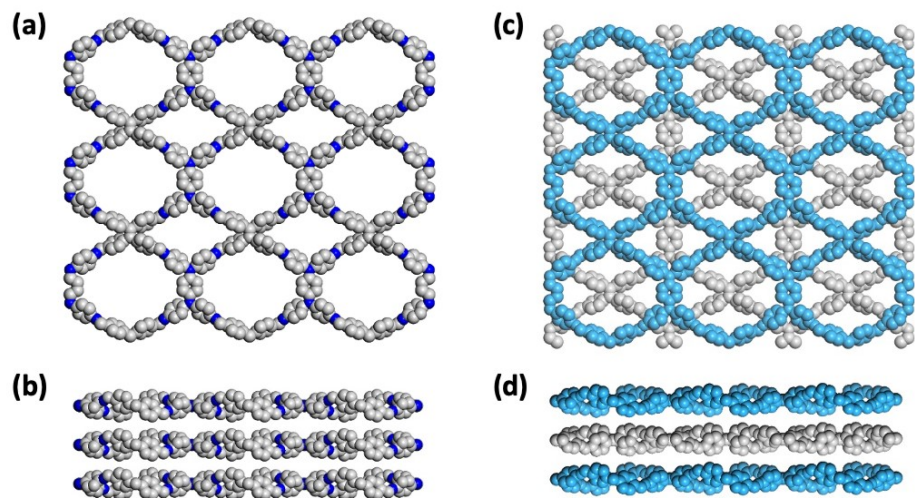


Fig. S7. (a) Top and (b) side views of AA stacking of COF. (c) Top and (d) side views of AB stacking of COF.

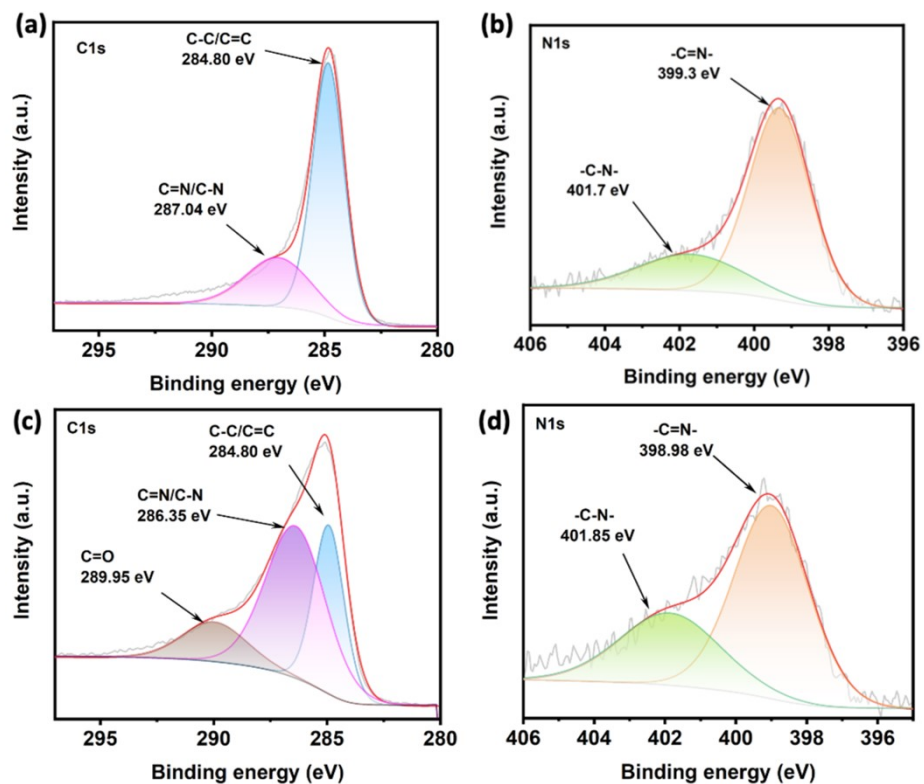


Fig. S8. High resolution XPS spectra of **(a)** C 1s and **(b)** N1s of COF, and **(c)** C 1s and **(d)** N1s of COF/CB8/AuNPs.

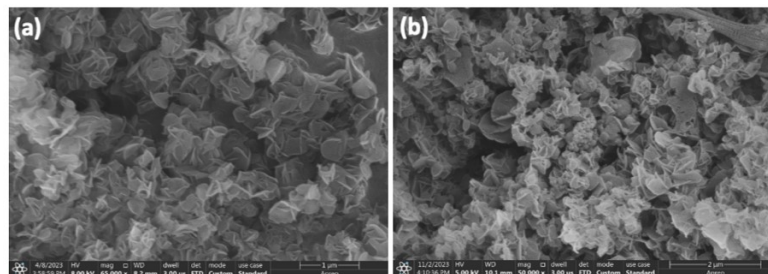


Fig. S9. SEM images of **(a)** COF and **(b)** COF/CB8/AuNPs.

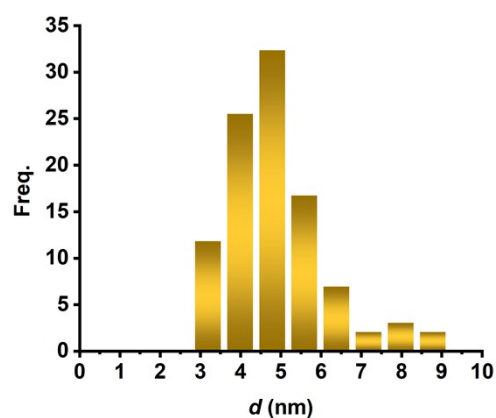


Fig. S10. Size distribution column of AuNPs in COF/CB8/AuNPs.

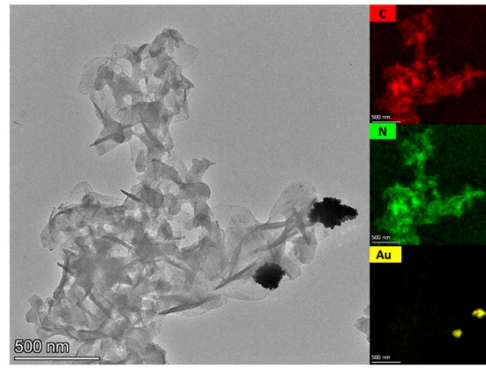


Fig. S11. TEM image and corresponding EDS elemental mappings of COF/AuNPs.

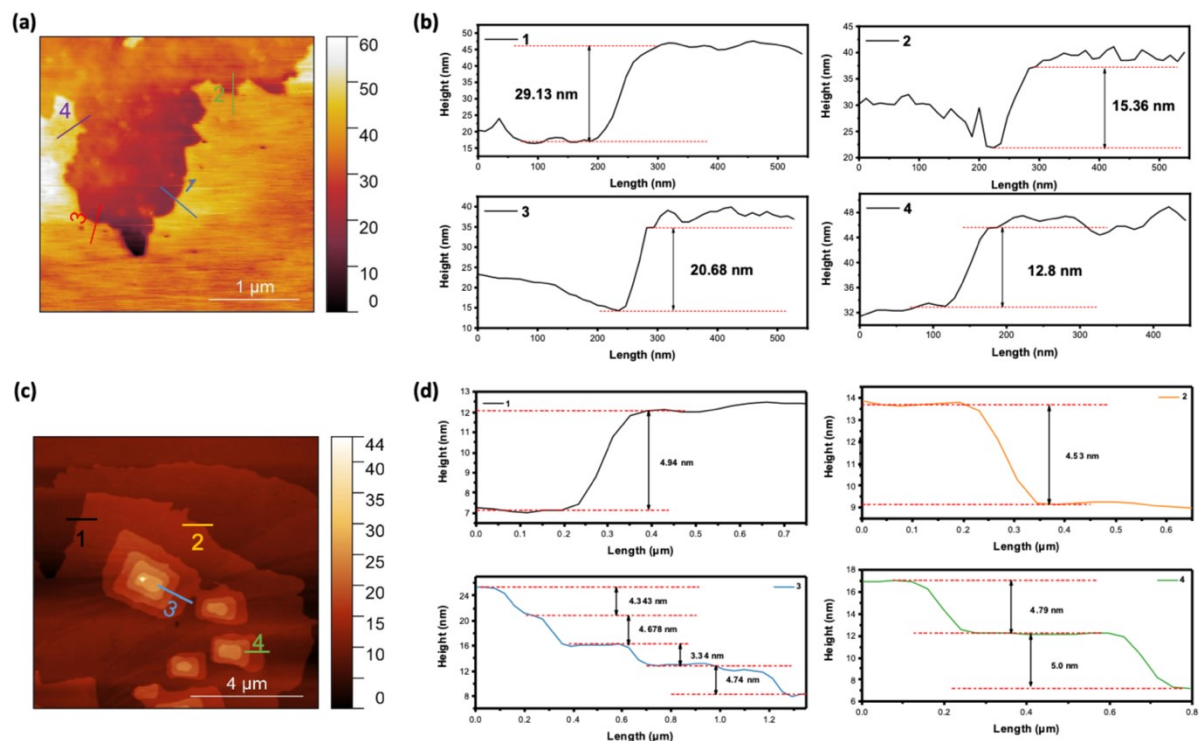


Fig. S12. AFM images of (a) COF and (c) COF/CB8/AuNPs, and corresponding height profiles of (b) COF and (d) COF/CB8/AuNPs.

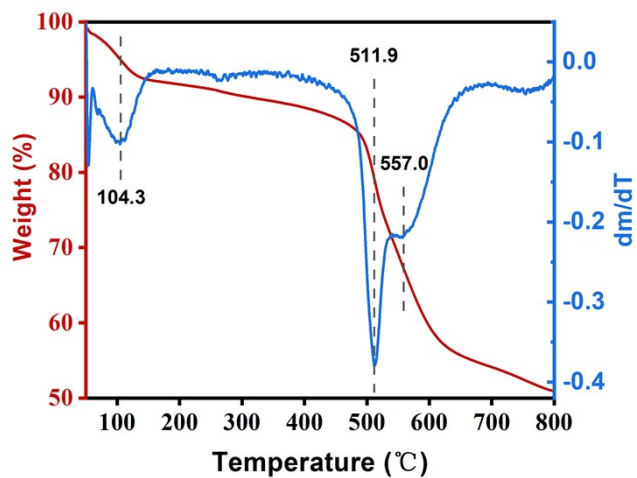


Fig. S13. TG-DTA spectra of COF.

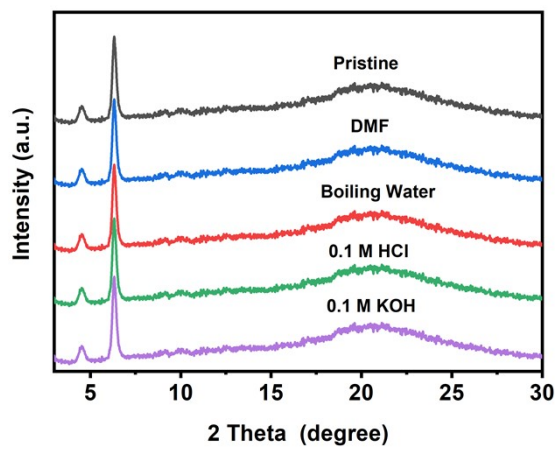


Fig. S14. PXRD patterns of pristine COF and after immersing in different solvents for seven days: DMF, boiling water, 0.1 M HCl and 0.1 M KOH.

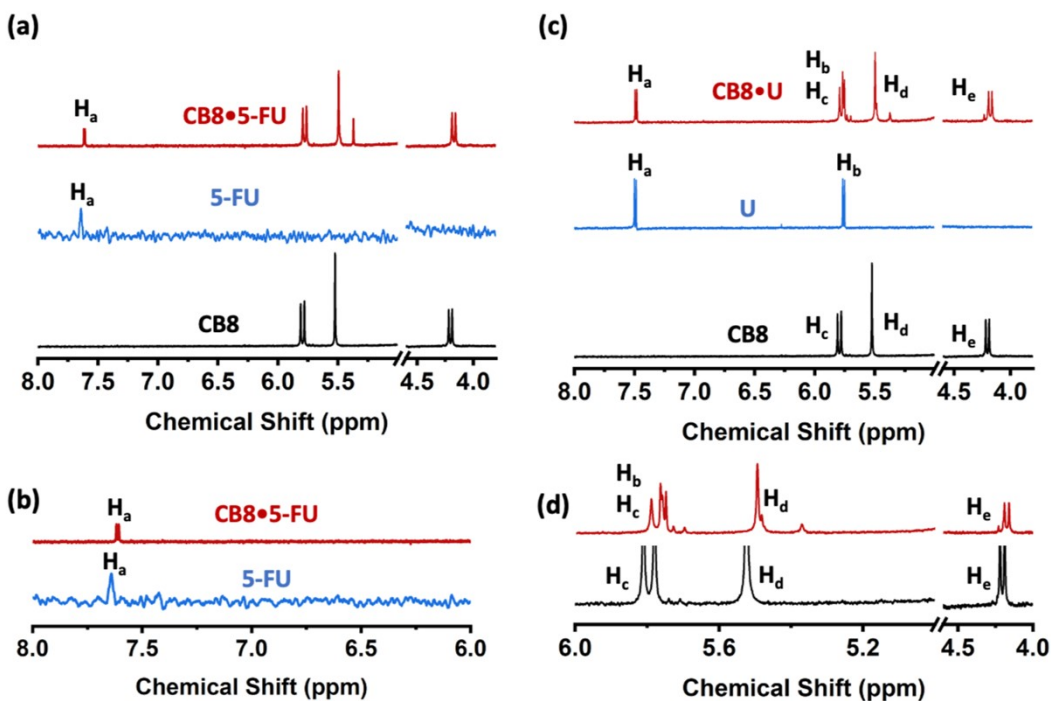


Fig. S15. (a) ¹H NMR and corresponding (b) zoom-in version of 1 mM CB8, 1 mM 5-FU and 1 mM CB8•5-FU in D_2O . (c) ¹H NMR and corresponding (d) zoom-in version of 1 mM CB8, 1 mM U and 1 mM CB8•U in D_2O .

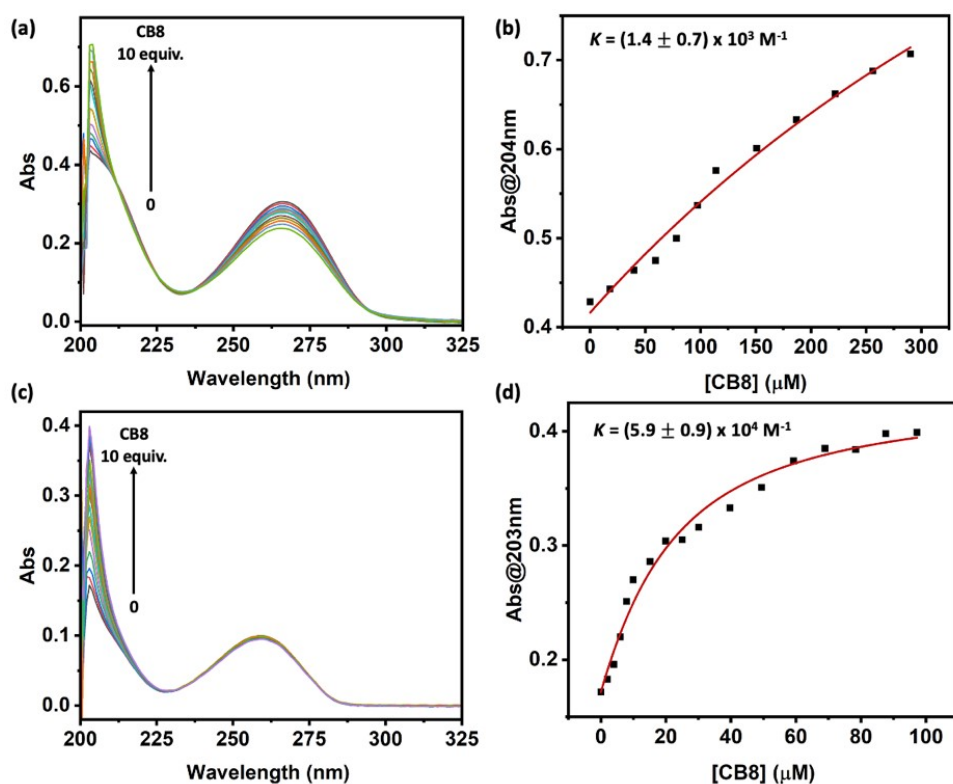


Fig. S16. (a) UV-vis spectra of 40 μM 5-FU with addition of CB8. (b) UV-vis titration fitting for binding constant estimation CB8•5-FU. (c) UV-vis spectra of 10 μM U with addition of CB8. (d) UV-vis titration fitting for binding constant estimation CB8•U.

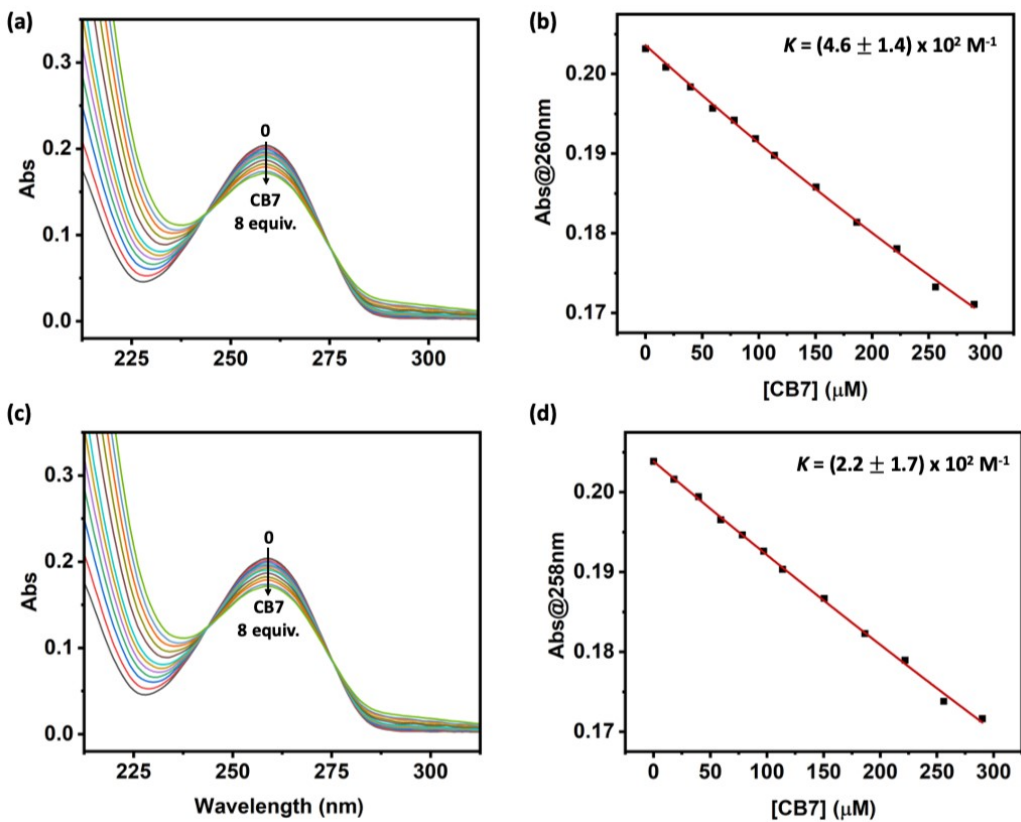


Fig. S17. (a) UV-vis spectra of 40 μM 5-FU with addition of CB7. (b) UV-vis titration fitting for binding constant estimation CB7•5-FU. (c) UV-vis spectra of 40 μM U with addition of CB7. (d) UV-vis titration fitting for binding constant estimation CB7•U.

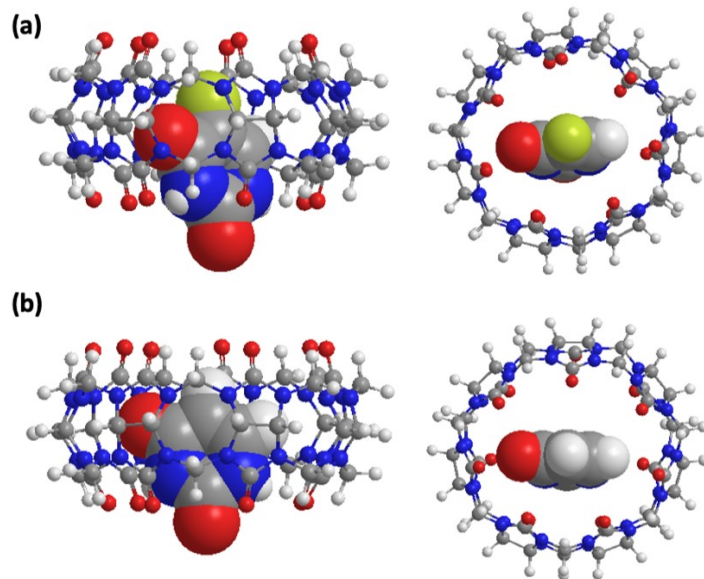


Fig. S18. DFT optimized molecular models (side and top view) of (a) CB7•5-FU and (b) CB7•U.

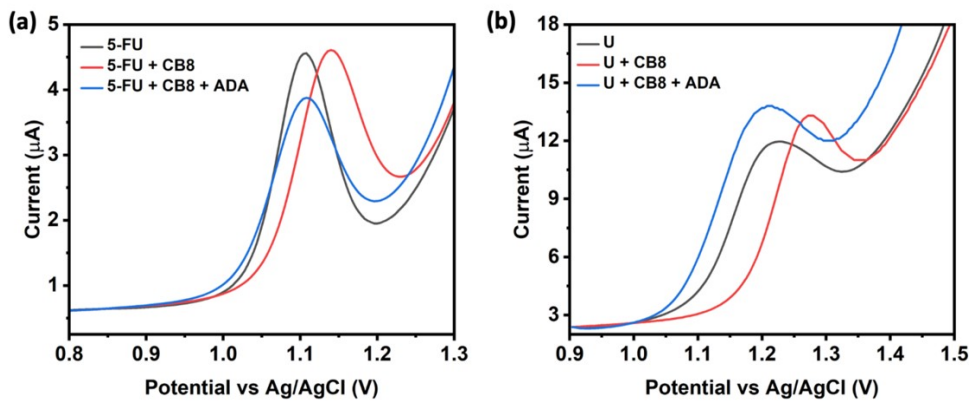


Fig. S19. Differential pulse voltammetric curves of (a) 0.4 mM 5-FU and (b) U in the absence and presence of 1 mM CB8 and 5 mM of 1-admantylamine (ADA) in 10 mM PBS using bare GCE as working electrode.

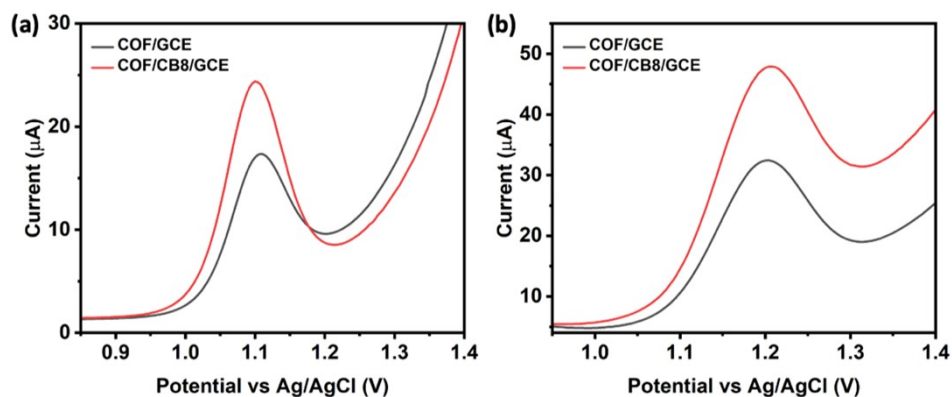


Fig. S20. Differential pulse voltammetric curves of (a) 5-FU and (b) U in 0.1 M PBS using COF/GCE and COF/CB8/GCE as working electrode.

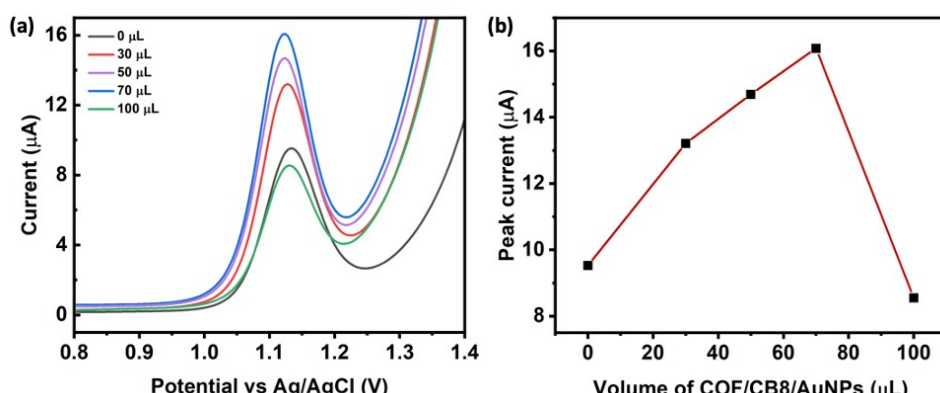


Fig. S21. (a) Differential pulse voltammograms of GCE modified by different volume of COF/CB8/AuNPs in 35 μ M 5-FU with 0.1 M PBS as supporting electrolyte. (b) Relationship between peak current of 5-FU and the volume of COF/CB8/AuNPs for GCE modification.

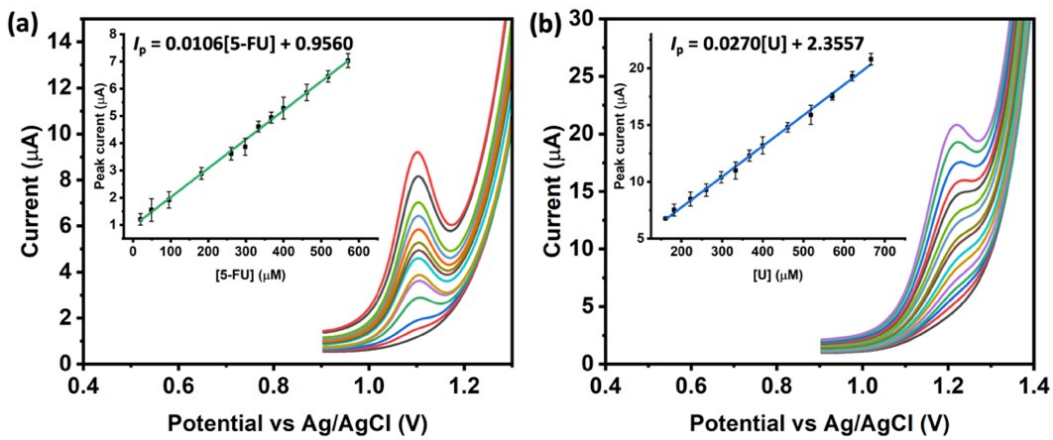


Fig. S22. Differential pulse voltammograms of bare GCE for detection towards (a) 5-FU and (b) U in 0.1 M PBS (pH 7.0).

Table S1. The comparison of sensing properties towards 5-FU and U by COF/CB8/AuNPs with previously reported modified electrodes in the literature.

Analyte	Electrode	Method	Linear detection range (μM)	LoD (μM)	Ref.
5-FU	AuNPs/MWCNT/GCE	DPV	0.03 ~ 10.0	0.02	[S1]
5-FU	Au/CS/PMAA/GCE	DPV	0.100 ~ 497	0.03	[S2]
5-FU	AgNPs/ PANINTs/ PGE	DPV	1.00 ~ 300	0.06	[S3]
5-FU	GQDs-PANI/ZnO-NCs/GCE	DPV	0.1 ~ 50	0.023	[S4]
5-FU	COF/CB8/AuNPs/GCE	DPV	0.8 ~ 58.4	0.037	<i>This work</i>
U	AMB MIP nanoarrays /Ag electrode	DPASV	0.01 ~ 2.49	0.0046	[S5]
U	NHSG/MIP/MWCNTs	DPASV	0.02 ~ 0.67	0.012	[S6]
U	PTH/MWCNTs/GCE	DPV	10 ~ 55000	0.2	[S7]
U	COF/CB8/AuNPs/GCE	DPV	0.5 ~ 62.0	0.074	<i>This work</i>

MWCNT: multiwall carbon nanotube. GCE: glassy carbon electrode. CS: chitosan. PMAA: poly(methacrylic acid). PANINTs: polyaniline nanotubes. PGE: pencil graphite electrode. GQDs-PANI/ZnO-NCs: graphene quantum dots-polyaniline/zinc oxide nanocomposites. PTH: poly (thionine). AMB: N-acryloyl-2-mercaptopbenzamide. MIP: molecularly imprinted polymers. NHSG: non-hydrolytic sol-gel.

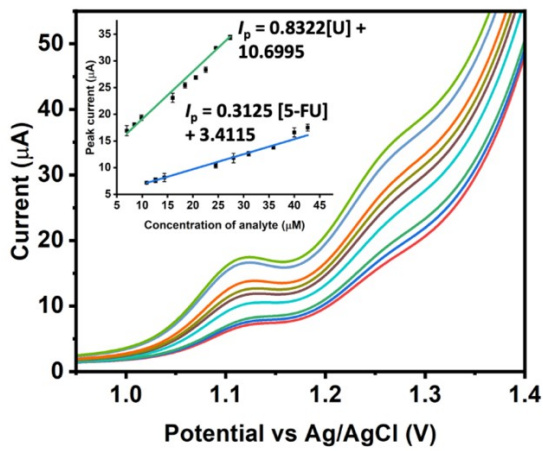


Fig. S23. Differential pulse voltammograms of COF/CB8/AuNPs/GCE for simultaneous detection of 5-FU and U in 0.1 M PBS.

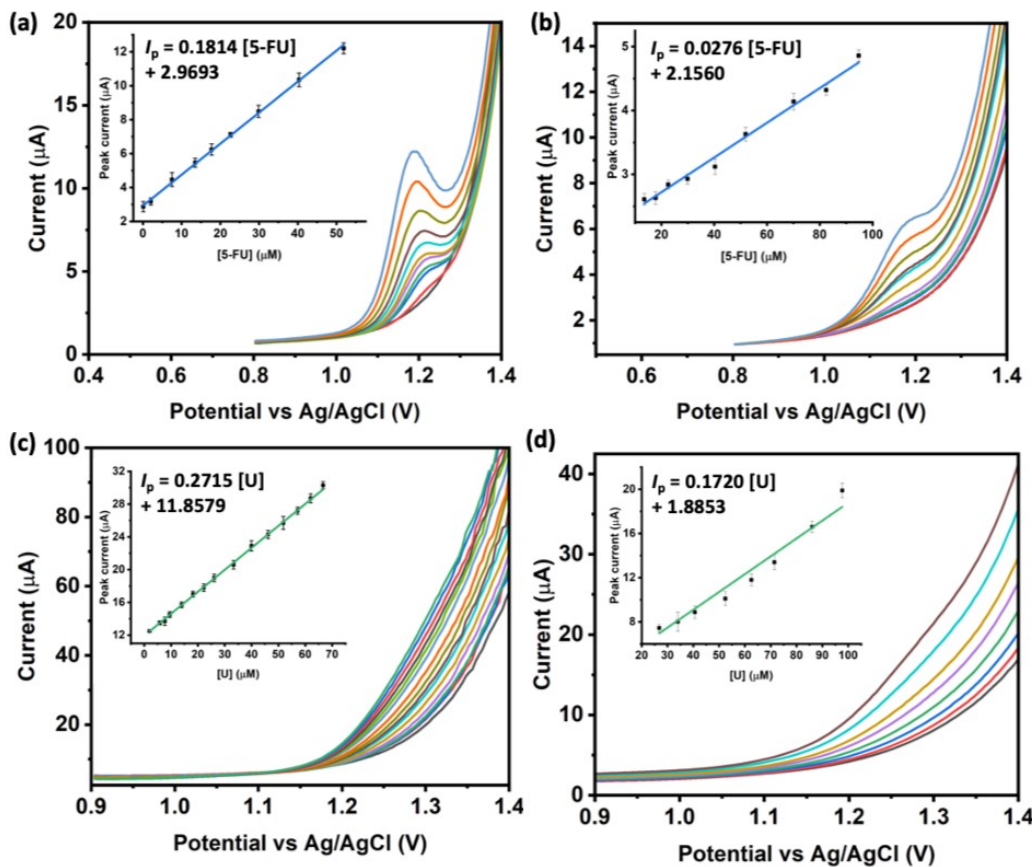


Fig. S24. Differential pulse voltammograms of COF/CB8/AuNPs/GCE for detection towards 5-FU in (a) native synthetic urine and (b) fetal bovine serum, and U in (c) native synthetic urine and (d) fetal bovine serum. Insets are calibration plots of U.

Table S2. Summary of sensing properties for simultaneous detection of 5-FU and U in different biofluids.

Matrix	Analyte	Regression equation	Linear detection range (μM)	LoD (μM)
PBS	5-FU	$I_p = 0.3125[5\text{-FU}] + 3.4115, R^2 = 0.9752$	10-43	0.041
	U	$I_p = 0.8322[U] + 10.6995, R^2 = 0.9788$	5-27	0.076
Native SU	5-FU	$I_p = 0.1732[5\text{-FU}] + 7.6756, R^2 = 0.9902$	16-51	0.074
	U	$I_p = 0.4166[U] + 16.7331, R^2 = 0.9363$	8-30	0.15
10x diluted FBS	5-FU	$I_p = 0.3127[5\text{-FU}] + 2.4379, R^2 = 0.9766$	17-62	0.041
	U	$I_p = 0.6523[U] + 14.7939, R^2 = 0.9824$	11-41	0.098

Table S3. Simulated atomic coordinates of COF.

Space group: P222			
3D orthorhombic; $a = 21.3 \text{ \AA}$, $b = 19.0 \text{ \AA}$, $c = 7.4016 \text{ \AA}$; $\alpha = \beta = \gamma = 90^\circ$			
Atom	x	y	z
C1	0.7458	0.14964	0.28937
C2	0.65335	0.14633	0.51935
C3	0.68091	0.12889	0.35157
C4	0.64596	0.08598	0.23327
C5	0.58692	0.05948	0.28063
C6	0.55963	0.0747	0.44873
C7	0.59309	0.11957	0.56719
N8	0.78411	0.1915	0.36452
C9	0.82923	0.76877	0.58823
C10	0.84482	0.7099	0.69456
C11	0.90151	0.67291	0.66804
C12	0.94473	0.69284	0.53214
C13	0.92921	0.75326	0.42852
C14	0.87249	0.79038	0.45593
C15	0.9438	0.53699	0.49276
H17	0.76103	0.12731	0.16204
H18	0.67873	0.17895	0.61444
H19	0.66507	0.07131	0.10289
H20	0.56289	0.02512	0.18641
H21	0.57381	0.13161	0.69894
H22	0.81409	0.694	0.80387
H23	0.9123	0.62958	0.75782
H24	0.96069	0.77127	0.32337
H25	0.86327	0.83716	0.37656
H26	0.8987	0.5623	0.47876
C27	0	0.57684	0.5
N28	0	0.6553	0.5
C29	0.5	0.96379	0.5

Reference

- [S1] Satyanarayana, M.; Goud, K. Y.; Reddy, K. K.; Gobi, K. V. Biopolymer Stabilized Nanogold Particles on Carbon Nanotube Support as Sensing Platform for Electrochemical Detection of 5-Fluorouracil in-vitro. *Electrochim. Acta* **2015**, *178*, 608-616.
- [S2] Vishnu S. K, D.; Ranganathan, P.; Rwei, S.-P.; Pattamaprom, C.; Kavitha, T.; Sarojini, P. New reductant-free synthesis of gold nanoparticles-doped chitosan-based semi-IPN nanogel: A robust nanoreactor for exclusively sensitive 5-fluorouracil sensor. *Int. J. Biol. Macromol.* **2020**, *148*, 79-88.
- [S3] Zahed, F. M.; Hatamluyi, B.; Lorestani, F.; Es'haghi, Z. Silver nanoparticles decorated polyaniline nanocomposite based electrochemical sensor for the determination of anticancer drug 5-fluorouracil. *J. Pharmaceut. Biomed. Anal.* **2018**, *161*, 12-19.
- [S4] Hatamluyi, B.; Es'haghi, Z.; Modarres Zahed, F.; Darroudi, M. A novel electrochemical sensor based on GQDs-PANI/ZnO-NCs modified glassy carbon electrode for simultaneous determination of Irinotecan and 5-Fluorouracil in biological samples. *Sens. Actuators, B* **2019**, *286*, 540-549.
- [S5] Prasad, B. B.; Kumar, A. Development of molecularly imprinted polymer nanoarrays of N-acryloyl-2-mercaptopbenzamide on a silver electrode for ultratrace sensing of uracil and 5-fluorouracil. *J. Mater. Chem. B* **2015**, *3*, 5864-5876.
- [S6] Prasad, B. B.; Kumar, D.; Madhuri, R.; Tiwari, M. P. Nonhydrolytic sol-gel derived imprinted polymer–multiwalled carbon nanotubes composite fiber sensors for electrochemical sensing of uracil and 5-fluorouracil. *Electrochim. Acta* **2012**, *71*, 106-115.
- [S7] Liu, H.; Wang, G.; Hu, J.; Chen, D.; Zhang, W.; Fang, B. Electrocatalysis and determination of uracil on polythionine/multiwall carbon nanotubes modified electrode. *J. Appl. Polym. Sci.* **2008**, *107*, 3173-3178.